HAL
open science

Numerical simulation of interaction of solitary deformation waves in microstructured solids

A. Salupere, K. Tamm, J. Engelbrecht

To cite this version:

A. Salupere, K. Tamm, J. Engelbrecht. Numerical simulation of interaction of solitary deformation waves in microstructured solids. International Journal of Non-Linear Mechanics, 2008, 43 (3), pp.201. 10.1016/j.ijnonlinmec.2007.12.011 . hal-00501770

HAL Id: hal-00501770

https://hal.science/hal-00501770v1

Submitted on 12 Jul 2010

HAL is a multi-disciplinary open access archive for the deposit and dissemination of scientific research documents, whether they are published or not. The documents may come from teaching and research institutions in France or abroad, or from public or private research centers.

L'archive ouverte pluridisciplinaire **HAL**, est destinée au dépôt et à la diffusion de documents scientifiques de niveau recherche, publiés ou non, émanant des établissements d'enseignement et de recherche français ou étrangers, des laboratoires publics ou privés.

Author's Accepted Manuscript

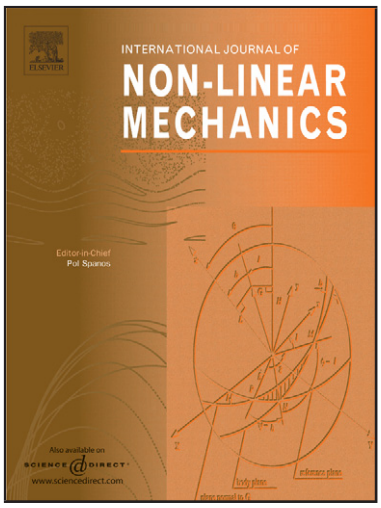

www.elsevier.com/locate/nlm

Numerical simulation of interaction of solitary deformation waves in microstructured solids

A. Salupere, K. Tamm, J. Engelbrecht

PII: S0020-7462(07)00233-8
DOI: doi:10.1016/j.ijnonlinmec.2007.12.011
Reference: NLM 1427

To appear in: *International Journal of Non-Linear Mechanics*

Received date: 25 May 2007
Revised date: 31 October 2007
Accepted date: 18 December 2007

Cite this article as: A. Salupere, K. Tamm and J. Engelbrecht, Numerical simulation of interaction of solitary deformation waves in microstructured solids, *International Journal of Non-Linear Mechanics* (2007), doi:10.1016/j.ijnonlinmec.2007.12.011

This is a PDF file of an unedited manuscript that has been accepted for publication. As a service to our customers we are providing this early version of the manuscript. The manuscript will undergo copyediting, typesetting, and review of the resulting galley proof before it is published in its final citable form. Please note that during the production process errors may be discovered which could affect the content, and all legal disclaimers that apply to the journal pertain.

ACCEPTED MANUSCRIPT

Numerical simulation of interaction of solitary deformation waves in microstructured solids

A. Salupere [a,b,*], K. Tamm [a,b], J. Engelbrecht [a]

[a] *Centre for Nonlinear Studies, Institute of Cybernetics at Tallinn University of Technology, Akadeemia tee 21, 12618, Tallinn, Estonia*

[b] *Department of Mechanics, Tallinn University of Technology, Ehitajate tee 5, 19086, Tallinn, Estonia*

Abstract

In the present paper 1D wave propagation in microstructured solids is modelled based on the Mindlin theory and hierarchical approach. The governing equation under consideration is nonintegrable therefore it is analysed numerically. Propagation and interaction of localised initial pulses is simulated numerically over long time intervals by employing the pseudospectral method. Special attention is paid to the solitonic character of the solution.

Key words: Microstructured solids, Mindlin model, Solitary waves, Solitons
PACS: 05.45.Yv, 46.40.Cd

Accepted manuscript

1. Introduction and model equations

Wide application of microstructured materials (like alloys, crystallites, ceramics, functionally graded materials, etc) in technology needs also proper testing methods in order to evaluate the properties of such materials. This need is especially acute because microstructural properties affect considerably the macrobehaviour of a compound material or a structure. In most general terms, microstructure means the existence of grains, inclusions, layers, block walls etc and the influence of anisotropy. There are powerful methods in continuum mechanics in order to describe the influence of such irregularities of media starting from early works of Cosserats and Voigt up to contemporary formulations. Corresponding models should be able to account for various scales of microstructure (see [1–4] and references therein). The scale-dependence involves dispersive as well as different nonlinear effects and if they are balanced then solitary waves and/or solitons may emerge.

Solitary waves in microstructured solids are analysed using different models (see [4–6] and references therein). However, the crucial point related to the derivation of governing equations is to distinguish between nonlinearities on macro- and microlevel together with proper modelling of dispersive effects. In [7–9] the Mindlin model [10] and hierarchical approach by Engelbrecht and Pastrone [4] is used in order to derive governing equations. By Mindlin [10], microstructured material is interpreted as an elastic continuum including microstructure that could be "a molecule of a polymer, a crystallite of a polycrystal or a grain of a granular material". This microstructure is modelled by microelements within the macrostructure. According to Eringen and Mindlin [1,10] fundamental balance laws should be formulated for macro- and microlevel separately. For 1D model this approach results in equations of motion in the following form:

* Corresponding author
Email addresses: salupere@ioc.ee (A. Salupere), kert@cens.ioc.ee (K. Tamm), je@ioc.ee (J. Engelbrecht).

ACCEPTED MANUSCRIPT

$$\begin{aligned} &\rho u_{tt} = \sigma_x, \\ &I\psi_{tt} = \eta_x - \tau. \end{aligned} \tag{1}$$

Here u is the macrodisplacement, ψ the microdeformation, ρ the macrodensity, I the microinertia, σ the macrostress, η the microstress and τ is the interactive force. The free energy function is considered in the following form:

$$\begin{aligned} &W = W_2 + W_3, \\ &W_2 = \frac{1}{2}au_x^2 + \frac{1}{2}B\psi^2 + \frac{1}{2}C\psi_x^2 + D\psi u_x, \\ &W_3 = \frac{1}{6}Nu_x^3 + \frac{1}{6}M\psi_x^3, \end{aligned} \tag{2}$$

where $a, B, C, D, M,\ N$ are constants. Here the quadratic term W_2 gives rise to the linear stress and the cubic W_3 — to the nonlinear part of stress. Then using the formulae

$$\sigma = \frac{\partial W}{\partial u_x}, \qquad \eta = \frac{\partial W}{\partial \psi_x}, \qquad \tau = \frac{\partial W}{\partial \psi} \tag{3}$$

eqs. (1) are expressed in terms of variables u and ψ

$$\begin{aligned} &\rho u_{tt} = au_{xx} + Nu_x u_{xx} + D\psi_x, \\ &I\psi_{tt} = C\psi_{xx} + M\psi_x\psi_{xx} - Du_x - B\psi. \end{aligned} \tag{4}$$

Next, slaving principle [4,7] is applied (in order to eliminate the microdeformation ψ from latter equations) and in terms of dimensionless variables $X = x/L,\ T = tc_0/L,\ U = u/U_0$, scale parameter $\delta = l^2/L^2$ (L and U_0 are amplitude and wavelength of the initial excitation, respectively; $c_0^2 = a/\rho$ and l is the scale of the microstructure) equations (4) result in the hierarchical model equation

$$\begin{aligned} &L_1 - \delta L_2 = 0 \\ &L_1 = U_{TT} - bU_{XX} - \frac{\mu}{2}\left(U_X^2\right)_X \\ &L_2 = \left(\beta U_{TT} - \gamma U_{XX} - \delta^{1/2}\frac{\lambda}{2}U_{XX}^2\right)_{XX} \end{aligned} \tag{5}$$

where L_1 is macrostructure wave operator and L_2 microstructure wave operator. New dimensionless material constants b, μ, β, γ and λ are introduced during change of variables and they are directly related to constants $a, B, C, D, M,\ N$ in free energy expression (2) (see [8,9] for details). If the scale parameter δ is small then the wave process is governed by properties of the macrostructure and vice-versa, if δ is large, then properties of the microstructure govern the process.

For future analysis eq. (5) is expressed in terms of deformation $v = U_X$ and lower-case letters x and t are used for dimensionless coordinate and time.

$$\begin{aligned} &v_{tt} - bv_{xx} - \frac{\mu}{2}\left(v^2\right)_{xx} - \\ &\delta\left(\beta v_{tt} - \gamma v_{xx}\right)_{xx} + \delta^{3/2}\frac{\lambda}{2}\left[\left(v_x\right)^2\right]_{xxx} = 0. \end{aligned} \tag{6}$$

The full derivation of governing equation (6) can be found in [7,8].

Equation (6) is nonintegrable but it is possible to find its travelling wave solution $v(x-ct)$ in the form of an asymmetric solitary wave using numerical integration under asymptotic boundary conditions (i.e. $u, u_x, u_{xx}, \ldots \to 0$, if $x \to \pm\infty$). The analytic conditions for the existence of solitary waves modelled by equation (6) are given by Janno and Engelbrecht in [8,9]:

$$\begin{aligned} &\frac{c^2-b}{\beta c^2-\gamma} > 0, \qquad \left(\frac{\beta c^2-\gamma}{c^2-b}\right)^3 > \frac{4\lambda^2}{\mu^2}, \\ &\mu \neq 0, \qquad \beta c^2 - \gamma \neq 0, \qquad c^2 - b \neq 0. \end{aligned} \tag{7}$$

In the case of $\lambda = 0$ the nonlinearity in the microscale is neglected and equation (6) admits bell-like solitary wave solution [6,9]

$$\begin{aligned} &v(x-ct) = A\,\mathrm{sech}^2\,\frac{\varkappa(x-ct)}{2}, \\ &A = \frac{3(c^2-b)}{\mu}, \quad \varkappa = \sqrt{\frac{c^2-b}{\delta(\beta c^2-\gamma)}}. \end{aligned} \tag{8}$$

From the viewpoint of soliton dynamics, three problems are of importance: the existence of solitary waves, the emergence of solitary waves and the interaction of solitary waves. The latter is important in order to prove the solitonic character of solitary waves, i.e. to understand whether solitary waves are able to propagate at constant speed and shape and to restore these quantities after interactions. If yes, these solitary waves are called solitons. Here in this paper the basic model is a two-wave equation with complicated dispersive and nonlinear terms. The existence of solitary waves is proved by Janno and Engelbrecht [8,9], the preliminary analysis of emergence of trains of solitary waves is presented in our earlier study [11] and here we present the preliminary results on interaction of solitary waves. The notion of solitary waves is used because the elastic interaction should prove whether these waves are solitons or not. As it is shown below, the problem is complicated and needs further analysis.

Accepted manuscript

ACCEPTED MANUSCRIPT

2. Statement of the problem and numerical technique

In the present paper the propagation and the interaction of localised initial pulses in microstructured materials (governed by equation (6)) is simulated numerically over long time intervals. Two goals are stated (i) to examine the solitonic character of the solution and (ii) to estimate the influence of the microlevel nonlinear parameter λ on the solution.

For this reason equation (6) is integrated numerically under localised initial conditions

$$v(x,0) = \sum_{i=1}^{2} A_i^0 \operatorname{sech}^2 \frac{\varkappa_i (x-\xi_i)}{2}, \qquad 0 \le x < 2k\pi. \tag{9}$$

Initial amplitudes A_i^0 and the widths $\varkappa_i$ $(i = 1, 2)$ correspond to different initial speeds $c_1 \neq c_2$, ξ_i are initial phase shifts, and k is integer. It is clear that in case $c_1 c_2 < 0$ head-on collision and in case of $c_1 c_2 > 0$ overtaking interaction takes place (if periodic boundary conditions are applied then this is true as in case $c_1 > c_2$ as well as in case $c_1 < c_2$).

For numerical integration discrete Fourier transform (DFT) based pseudospectral method (PsM) [12,13] is used and therefore periodic boundary conditions

$$v(x,t) = v(x + 2k\pi, t) \tag{10}$$

are applied.

In a nutshell, the idea of the PsM is to approximate space derivatives making use of DFT and then to use standard ODE solvers for integration with respect to the time. Due to the mixed partial derivative term $\delta\beta v_{ttxx}$ the model equation (6) can not be directly integrated by PsM. Therefore we introduce new variable

$$\Phi = v - \delta\beta v_{xx}. \tag{11}$$

In terms of DFT the latter can be presented in the form

$$\Phi = F^{-1}[(1 + \delta\beta\omega^2)F(v)], \tag{12}$$

where F denotes the DFT, F^{-1} the inverse DFT and $\omega = \pm 1, \pm 2, \ldots \pm (N/2 - 1), -N/2,$. Then variable v and its spatial derivatives are expressed in terms of the variable Φ

$$\begin{aligned} v &= F^{-1}\left[\frac{F(\Phi)}{1+\delta\beta\omega^2}\right], \\ \frac{\partial^n v}{\partial x^n} &= F^{-1}\left[\frac{(i\omega)^n F(\Phi)}{1+\delta\beta\omega^2}\right]. \end{aligned} \tag{13}$$

Finally, equation (6) can be rewritten in terms of variable Φ

$$\Phi_{tt} = \left[bv + \frac{\mu}{2}v^2 - \delta\gamma v_{xx} - \delta^{3/2}\frac{\lambda}{2}(v_x^2)_x\right]_{xx} \tag{14}$$

(v and its space derivatives are calculated making use of expressions (12) and (13)). In order to simulate the propagation and the interaction of localised pulses equation (14) is solved numerically by PsM under initial and boundary conditions (9) and (10), respectively.

Calculations are carried out using SciPy package [14]: for DFT the FFTW [15] library and for ODE solver the F2PY [16] generated Python interface to ODEPACK Fortran code [17] is used.

3. Results and discussion

In the present Section two different head-on interaction cases are considered. In the first case solitary waves of equal amplitude propagate at equal initial speed in opposite directions ($c_1 = -c_2 = 0.9$) and in the second case solitary waves of different amplitude propagate at initial speeds $c_1 = 0.9$ and $c_2 = -0.9115$. Five parameters for equation (6) are fixed: $b = 0.7683$, $\mu = 0.125$, $\delta = 9$, $\beta = 7.6452$, $\gamma = 6.1825$, but λ has three different values 0, 0.0025, and 0.005. For $|c_i| = 0.9115$ and $|c_i| = 0.9$ conditions (7) are satisfied for all considered values of parameter λ. We stress here that if conditions (7) are satisfied, then travelling wave solutions in the form of single asymmetric solitary wave can exist for equation (6) [8,9]. Numerical integration is carried out for $0 \le t \le 6000$, waveprofiles are saved at every $\Delta t = 0.5$, the length of the space period is 60π and the number of space-grid points is $n = 1024$. According to expression $(8)_2$ amplitude $A = 1.00$ corresponds to the speed $|c_i| = 0.9$ and amplitude $A = 1.50$ to the speed $|c_i| = 0.9115$. In all considered cases amplitudes of solitary waves increase during interactions and decrease after interactions. If initial amplitudes, shapes and velocities are restored after interactions — like in case of Boussinesq models — then such solitary waves can be called solitons.

In [18] the same interaction types were studied for remarkably shorter time intervals ($0 \le t \le 500$). For the equal initial amplitude case the length of the space interval was 24π and in the case of nonequal amplitudes 96π. It was found that for $\lambda = 0$ and for relatively small values of parameters the behaviour of solitary waves was very close to that of solitons

Accepted manuscript

ACCEPTED MANUSCRIPT

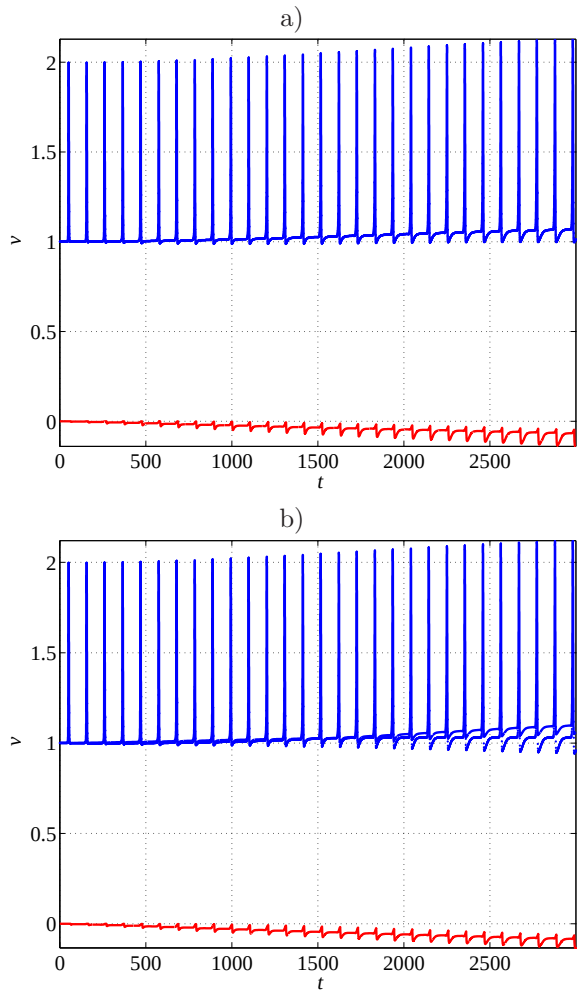

Fig. 1. Wave-profile maxima and minimum against time in case of $c_1 = -c_2 = 0.9$: a) $\lambda = 0$; b) $\lambda = 0.005$.

for the considered time and space intervals. Interaction between equal amplitude solitary waves was found to take place without phase shifts, but if interacting waves have different amplitude, then both were phase-shifted.

3.1. *Head-on collision of solitary waves with equal amplitudes*

In the present Subsection the interaction between two solitary waves having initial velocities are $c_1 = -c_2 = 0.9$ and equal initial amplitudes $A_0 = 1.00$ is studied. In Fig. 1, waveprofile maxima (heights) are plotted against time for two different values of parameter λ. In the beginning of the integration interval ($t < 500$) height at "peaks" of interaction A^i ("peaks" of interaction correspond to local max-

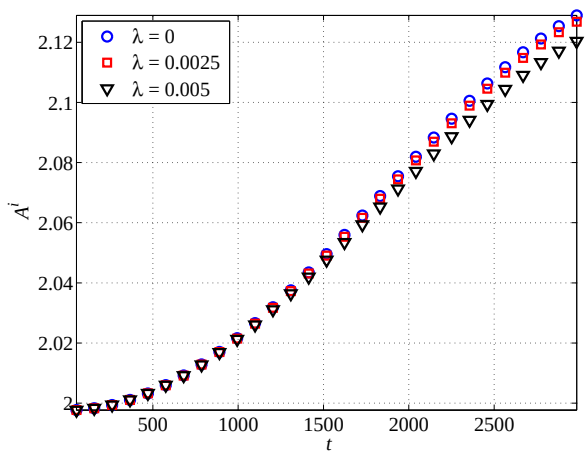

Fig. 2. Amplitude at "peaks" of interactions A^i against time in case of $c_1 = -c_2 = 0.9$.

ima of amplitude curves in Fig. 1) is close to double initial amplitude of interacting solitary waves. However for $t > 500$ the amplitude A^i increases apparently, cf. Fig. 2 where the amplitude A^i is plotted against time for different values of λ. For $t < 1000$ all three curves practically coincide, but for higher values of t they diverge essentially — the higher the value of λ the lower the values of A^i. At $t = 3000$ the value of A^i is more than 6% higher than double initial amplitude of interacting solitary waves for all three values of λ.

The length of time intervals between "peaks" of interaction does not depend on λ and is between values 104.63 and 104.71. It is clear from Fig. 1 that for $t < 500$ interacting solitary waves more or less restore their initial heights for certain time intervals. However, for higher values of t such a phenomenon does not take place. Furthermore, for $\lambda > 0$ right-propagating and left-propagating solitary waves have different heights A_R and A_L between interactions. In Fig. 3 averaged amplitudes A_R^a and A_L^a are plotted against the number of interactions. Values of A_R^a and A_L^a after $k-$th interaction are obtained by averaging amplitudes of right- and left-propagating solitary waves over time intervals where both amplitudes have near constant values between kth and $(k+1)$th interaction (cf. Fig. 1). Analysis of single waveprofiles and data in Fig. 3 demonstrate that for $\lambda > 0$ amplitude $A_R^a > A_L^a$ until 15th interaction and *vice versa* $A_R^a < A_L^a$ after 15th interaction. The higher the value of λ the higher the amplitude A_L and the lover the amplitude A_R at $t = 3000$. This phenomenon depicts the behaviour at the given set of parameters and the critical value

Accepted manuscript

ACCEPTED MANUSCRIPT

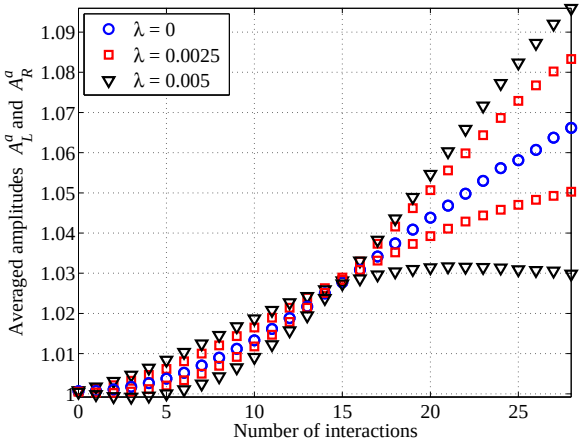

Fig. 3. Averaged amplitudes between interactions A_R^a and A_L^a against the number of interactions in case of $c_1 = -c_2 = 0.9$.

can be changed at other sets. It is evident that the averaged amplitudes tend to certain limits at larger number of interactions. The fact that amplitudes are not restored after interactions indicates that interactions between solitary waves are not elastic, i.e., a certain exchange of energy takes place between solitary waves during interaction. One can see below that the initial symmetric shape of solitary waves is also altered during interactions.

Between interactions both solitary waves propagate practically at initial speed. In order to estimate phase shifts during interactions the actual trajectories of solitary waves are compared with straight lines $x_i = \xi_i \pm 0.9t$, i.e., with phase-shift free trajectories (ξ_i are initial phase shifts, cf. (9)). In Fig. 4 cumulative phase shift in space is plotted against the number of interactions. The cumulative phase shift is calculated as average deviation between two considered trajectories over time interval $t_k + 25 \le t \le t_{k+1} - 25$, (time moments t_k and t_{k+1} correspond to kth and $(k+1)$th interaction, respectively). For the case $\lambda = 0$ both waves are shifted by the same extent and the cumulative phase shift after 28th interaction is about 0.81 which is 0.43% of the length of the space period. For $\lambda > 0$ phase-shifts for right-propagating and left-propagating solitary waves are different — right-propagating solitary wave is less phase-shifted than that of the left-propagating. However, compared to the length of the space period the cumulative phase-shift is less than 1% in all considered cases.

Janno and Engelbrecht have shown in [8,9] that for equation (6) exists symmetric bell-shaped travelling wave solution for $\lambda = 0$ and asymmetric travelling wave solution — for $\lambda > 0$. In our numerical experiments single solitary wave (8) propagates at constant amplitude and speed in case of $\lambda = 0$. In case of $\lambda > 0$ the initial symmetric solitary wave is deformed to that of asymmetric. Numerical analysis of interactions of solitary waves (8) demonstrate that due to interactions initial symmetric solitary waves are deformed to that of asymmetric even in case $\lambda = 0$. This phenomenon can be observed in

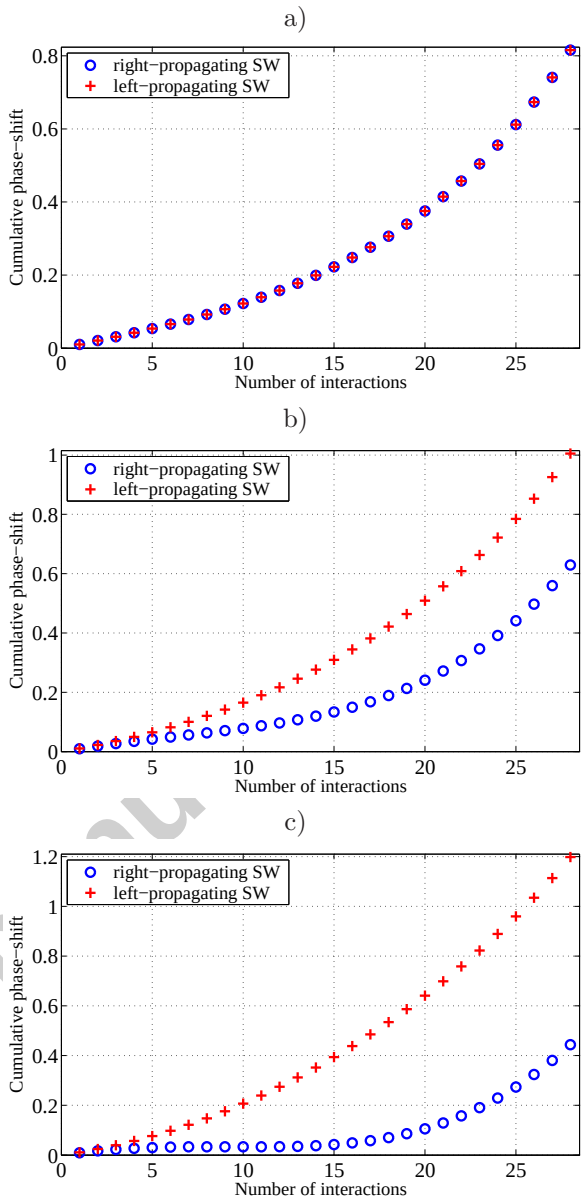

Fig. 4. Cumulative phase-shift of left- and right-propagating solitary waves against the number of interactions in case of $c_1 = -c_2 = 0.9$: a) $\lambda = 0$; b) $\lambda = 0.0025$; c) $\lambda = 0.005$

.

Accepted manuscript

ACCEPTED MANUSCRIPT

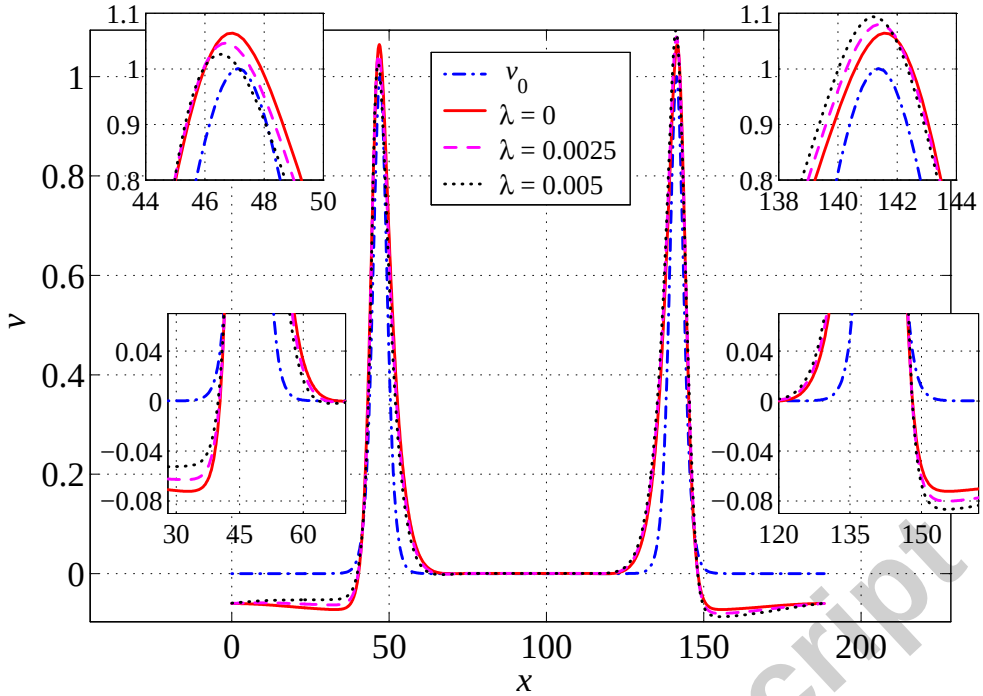

Fig. 6. Initial waveprofile and maximally separated waveprofiles after 28th interaction in case of $c_1 = -c_2 = 0.9$.

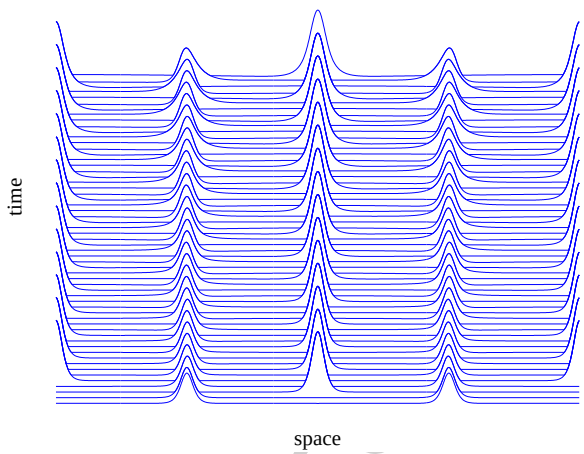

Fig. 5. Timeslices of wave-profiles at t=0, at interaction "peaks" and at time moments when two solitary waves are maximally separated in case of $c_1 = -c_2 = 0.9$ and $\lambda = 0$.

Fig. 5 where maximally separated waveprofiles are plotted besides waveprofiles at interaction "peaks". The asymmetry of solitary waves is clearly visible in Fig. 6 where solitary waves are plotted at $t = 0$ and at time moment when they are maximally separated after 28th interaction (the left solitary wave is propagating to the right and the right one to the left). It is clear that the higher the value of λ, the more asymmetric is the corresponding wave. Due to the asymmetry both waves are partly located below zero. Physically such a phenomenon can be interpreted as region of depression ($v > 0$ correspond to compression). The depression region is always located behind the propagating wave and the more interactions have taken place the stronger it is (cf. wave-profile minimum curve in Fig. 1).

3.2. *Head-on collision of solitary waves with nonequal amplitudes*

In the present Subsection we discuss interactions between two solitary waves having initial amplitudes $A_1^0 = 1.00$ and $A_2^0 = 1.50$ and initial velocities $c_1 = 0.9$ and $c_2 = -0.9115$. In Fig. 7 amplitude curves are plotted for $\lambda = 0$ and $\lambda = 0.005$. In the beginning of the integration interval the amplitude of waves at "peak" of interactions A^i is close to the sum of initial amplitudes like in the previous case. However, unlike the previous case the amplitude A^i is decreasing during the integration time interval. In Fig. 8 amplitudes A^i are plotted against time for three different values of parameter λ. The higher the value of λ the larger the decrease of the amplitude A^i. The length of time intervals between "peaks" of interaction does not depend on λ (like in the previous case)

ACCEPTED MANUSCRIPT

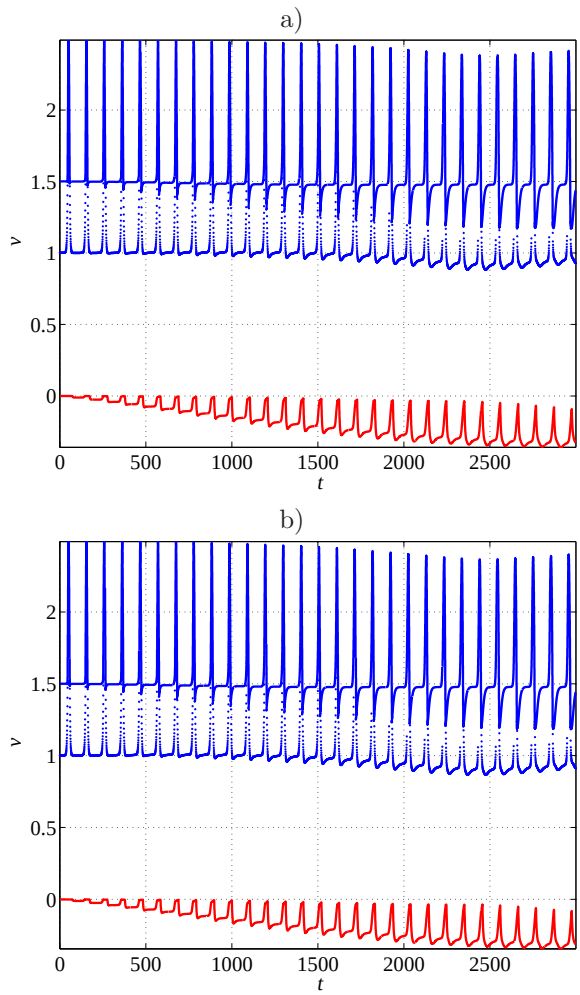

Fig. 7. Wave-profile maxima and minimum against time in case of $c_1 = 0.9$ and $c_2 = -0.9115$: a) $\lambda = 0$; b) $\lambda = 0.005$.

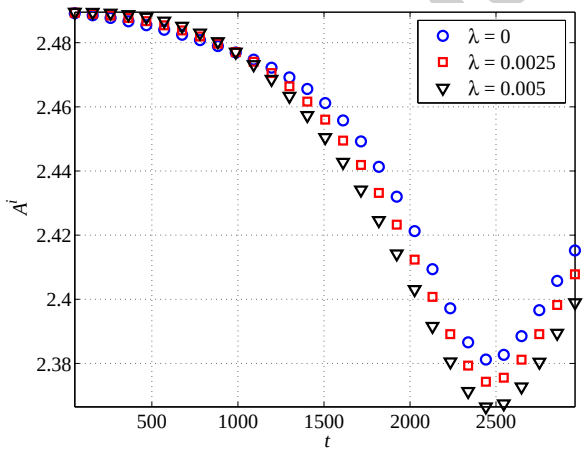

Fig. 8. Amplitudes at "peaks" of interactions in case of $c_1 = 0.9$ and $c_2 = -0.9115$.

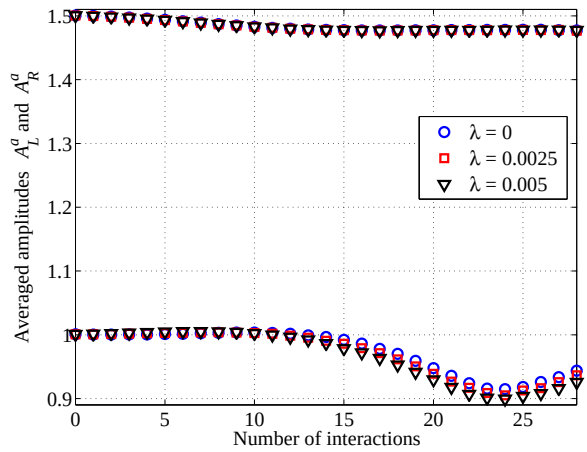

Fig. 9. Average amplitude between interactions in case of $c_1 = 0.9$ and $c_2 = -0.9115$.

and is now between values 103.35 and 104.00.

The behaviour of the higher (left-propagating) solitary wave between interactions is practically independent on the value of the parameter λ — after the first interaction the initial amplitude is practically restored, but then the average amplitude A_L^a decreases and after the 15th interaction near $t = 1500$ retains constant value (see Figs. 7 and 9). The amplitude of the lower (right-propagating) solitary wave behaves between interactions just the other way round — the amplitude A_R^a is practically constant in the beginning of the interaction interval and starts to decrease after the 12th interaction near $t = 1200$. Furthermore, up to the 12th interaction the right-propagating solitary wave practically restores its initial height.

Both solitary waves propagate between interaction at initial speed and we calculate the cumulative phase shift in the same way like in the previous case. Results are presented in Fig. 10 for three values of parameter λ. In the present case the maximal value of the cumulative phase shift is near nine (in previous case it was up to 1.2). Up to the 21st interaction the left-propagating, i.e., the higher solitary wave is more phase shifted than that of the right-propagating for all three values of λ. After that the cumulative phase shift for the right-propagating, i.e., the lower solitary wave increases rapidly from the value near 2.5 up to the value near 9 without reference to the value of the parameter λ.

The larger the number of interactions the more asymmetric is the lower solitary wave. Due to the asymmetry, the part of the waveprofile behind it is located below zero like in the previous case. For

ACCEPTED MANUSCRIPT

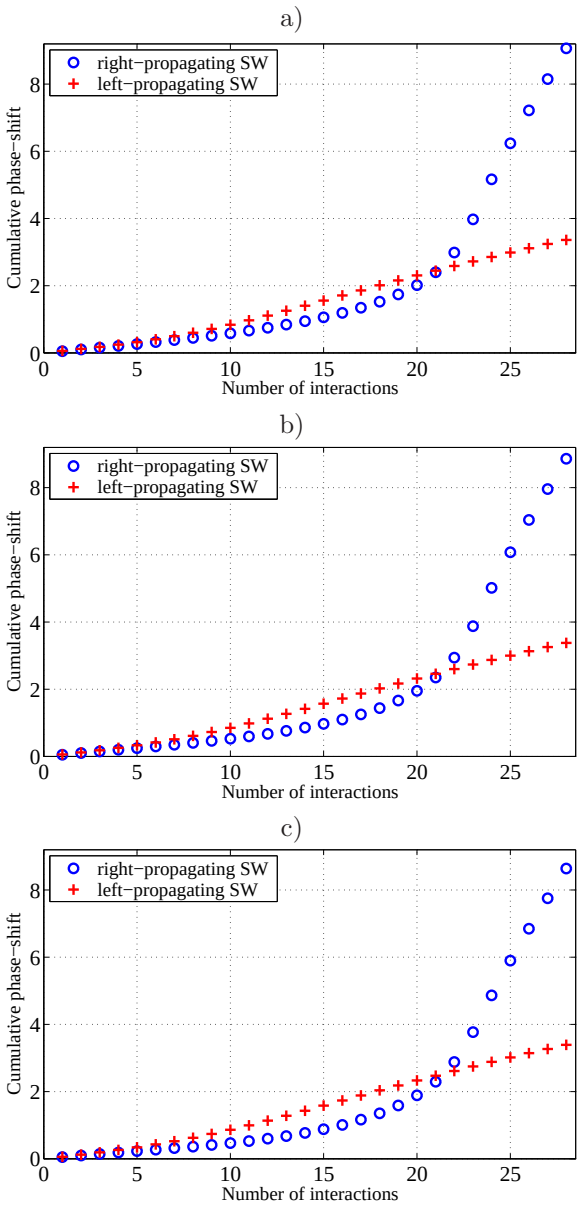

Fig. 10. Phase-shifts of left and right going solitary waves in case of $c_1 = 0.9$ and $c_2 = -0.9115$: a) $\lambda = 0$; b) $\lambda = 0.0025$; c) $\lambda = 0.005$

higher values of t waveprofile minimum has values close to zero only for very short time intervals near "peaks" of interactions (Fig. 7). In Fig. 11 solitary waves are plotted at $t = 0$ and at time moment when they are maximally separated after 28th interaction (the left solitary wave is propagating to the right and the right one to the left) for three values of λ. In the present case parameter λ has very weak influence on the shape of the waveprofile — amplitude of the lower solitary wave decreases slightly when λ increases, but one can not distinct three profiles in case of the higher solitary wave.

4. Conclusions

Well known and widely used evolution equations (Korteweg–de Vries equation and its modifications for example) are one-wave equations (the order of time derivative is one), i.e., they are able to govern only overtaking interactions of solitary waves. Equation (6) (used in the present paper) is a two-wave equation (the order of time derivative is two) and therefore gives us possibility to analyse also head-on collisions of waves.

In case of $\lambda = 0$ single symmetric bell-like solitary wave (8) is an analytical solution of equation (6) and it propagates with a constant speed and shape. Our numerical simulations have demonstrated that in case of $\lambda > 0$ the symmetric shape of initial single bell-like solitary wave (8) is altered to asymmetric shape during propagation. In the present paper the head-on collision of two sech^2-shape localised initial pulses is studied in case of $\lambda = 0$ as well as $\lambda > 0$. Material parameters for equation (6) and initial conditions (9) were chosen according to to conditions (7), i.e., for all considered sets of parameters travelling wave solutions in the form of single asymmetric solitary wave can exist for equation (6).

Main results are the following:

- Interactions between solitary waves are not complitely elastic even in case of $\lambda = 0$ — during interactions the symmetric shape of initial waves is altered to that of asymmetric. In case of $\lambda = 0$ and $A_1^0 = A_2^0$ the asymmetry is very weak after very first interactions. However, the higher the number of interactions, the more distinctive the asymmetry without reference to the values of parameter λ and initial velocities. In case of $A_1^0 \neq A_2^0$ the shape of the higher solitary wave is altered only slightly, but that of the lower one significantly.
- The asymmetry of the pulse is reflected in the altering of the shape of compression region of the pulse ($v > 0$) as well as in the emergence of depression zone ($v < 0$) beside that of compression. This phenomenon is more distinctive in case of $A_1^0 \neq A_2^0$.
- Phase shifts, characteristic for soliton type interactions, can be easily traced in case of $A_1^0 \neq A_2^0$. In case of $A_1^0 = A_2^0$ even the cumulative phase shift over long time intervals is small compared

ACCEPTED MANUSCRIPT

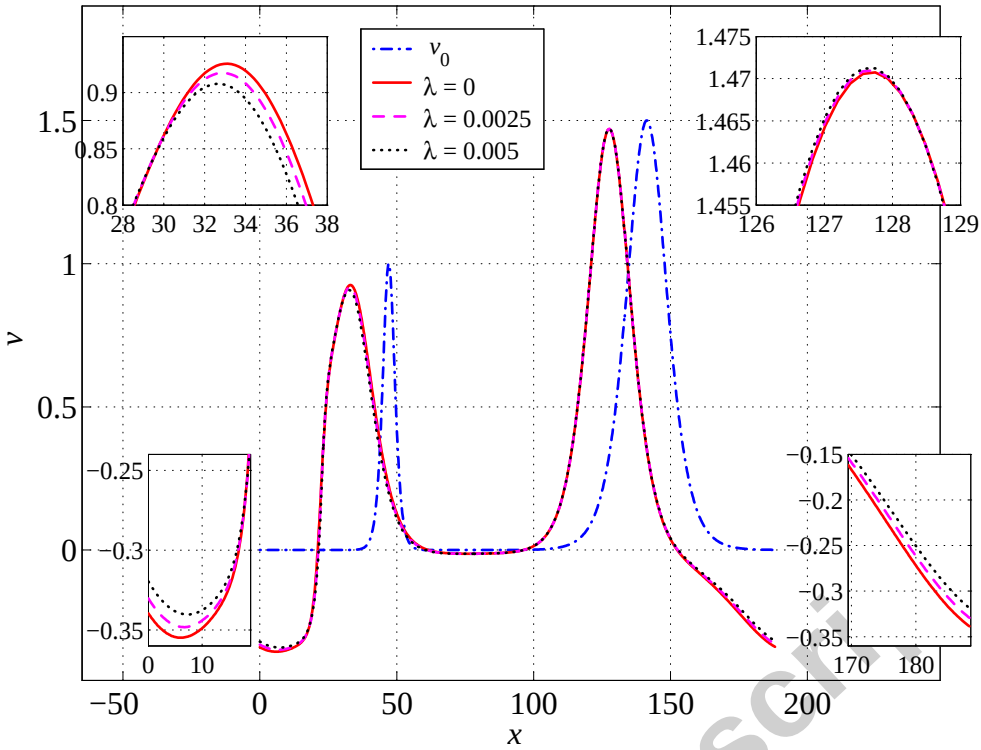

Fig. 11. Initial waveprofile and maximally separated waveprofiles after 28th interaction in case of $c_1 = 0.9$ and $c_2 = -0.9115$.

to the considered space interval and/or distance traveled by interacting waves.

– In the beginning of the integration interval the heigth (amplitude) of interacting waves is practically restored between interactions. For higher values of t the heigth can be altered remarkably. In case of $A_1^0 = A_2^0$ heights of right- and left-propagating waves are restored on unequal levels.
– The nonlinearity of the microstructure (parameter λ) has stronger influence on the character of solution in the case of equal initial amplitudes $A_1^0 = A_2^0$ (cf. set of Figs. 1–4, 6 with Figs. 7–11).
– Over short time intervals and small number of interactions the behaviour of the solution is very close to the solitonic behaviour in all consdered cases. The higher the number of interactions and the longer the time interval the more the initial and the restored waveprofiles differ.

In order to explain phenomena described in this paper in more detail, a furthure analysis based on energy distribution and spectral changes is needed. Clearly, two-wave interactions differ from one-wave interactions. The special analysis of one-wave interactions is presented in [19,20], the same should be done for this model.

Acknowledgements

The financial support from the Estonian Science Foundation (Grants No 5565 and 7035) is gratefully acknowledged.

References

[1] A. Eringen, Microcontinuum Field Theories. I Foundations and Solids, Springer, New York, 1999.
[2] R. Phillips, Crystals, Defects and Microstructures. Modelling Across Scales, Cambridge University Press, Cambridge, 2001.
[3] G. Maugin, Nonlinear Waves in Elastic Crystals, Oxford Univ. Press, Oxford, 1999.
[4] J. Engelbrecht, F. Pastrone, Waves in microstructured solids with nonlinearities in microscale, Proc. Estonian Acad. Sci. Phys. Math. 52 (1) (2003) 12–20.
[5] V. I. Erofeev, Wave Processes in Solids with Microstructure, World Scientific, Singapore, 2003.
[6] A. V. Porubov, Amplification of Nonlinear Strain Waves in Solids, World Scientific, Singapore, 2003.
[7] J. Engelbrecht, A. Berezovski, F. Pastrone, M. Braun, Waves in microstructured materials and dispersion, Phil. Mag. 85 (2005) 4127–4141.
[8] J. Janno, J. Engelbrecht, Solitary waves in nonlinear microstructured materials, J. Phys. A: Math. Gen. 38 (2005) 5159–5172.

Accepted manuscript

ACCEPTED MANUSCRIPT

[9] J. Janno, J. Engelbrecht, An inverse solitary wave problem related to microstructured materials, Inverse Problems 21 (2005) 2019–2034.
[10] R. D. Mindlin, Micro-structure in linear elasticity, Arch. Rat. Mech. Anal. 16 (1964) 51–78.
[11] J. Engelbrecht, A. Berezovski, A. Salupere, Nonlinear deformation waves in solids and dispersion, Wave Motion 44 (6) (2007) 493–500.
[12] B. Fornberg, A Practical Guide to Pseudospectral Methods, Cambridge University Press, Cambridge, 1998.
[13] A. Salupere, J. Engelbrecht, P. Peterson, On the long-time behaviour of soliton ensembles, Mathematics and Computers in Simulation 62 (2003) 137–147.
[14] E. Jones, T. Oliphant, P. Peterson, et al., SciPy: Open source scientific tools for Python, http://www.scipy.org (2001).
[15] M. Frigo, S. G. Johnson, The design and implementation of FFTW3, Proceedings of the IEEE 93 (2) (2005) 216–231.
[16] P. Peterson, F2PY: Fortran to python interface generator, http://cens.ioc.ee/projects/f2py2e/ (2005).
[17] A. C. Hindmarsh, Odepack, a systematized collection of ODE solvers, in: R. S. Stepleman, et al. (Eds.), Scientific Computing, North-Holland, Amsterdam, 1983, pp. 55–64.
[18] A. Salupere, K. Tamm, J. Engelbrecht, P. Peterson, On interaction of deformation waves in microstructured solids, Proc. Estonian Acad. Sci. Phys. Math. 56 (2) (2007) 93–99.
[19] A. Salupere, J. Engelbrecht, P. Peterson, Long-time behaviour of soliton ensembles. Part I—Emergence of ensembles, Chaos, Solitons & Fractals 14 (2002) 1413–1424.
[20] A. Salupere, J. Engelbrecht, P. Peterson, Long-time behaviour of soliton ensembles. Part II—Periodical patterns of trajectories, Chaos, Solitons & Fractals 15 (2003) 29–40.

Accepted manuscript